



HAL
open science

Crystalline and Glassy Phases in the Ternary System Tl/Bi/Cl: Synthesis and Crystal Structures of the Thallium(I) Chloridobismutates(III) Tl_3BiCl_6 and $TlBi_2Cl_7$

Johannes Beck, Sebastian Benz

► **To cite this version:**

Johannes Beck, Sebastian Benz. Crystalline and Glassy Phases in the Ternary System Tl/Bi/Cl: Synthesis and Crystal Structures of the Thallium(I) Chloridobismutates(III) Tl_3BiCl_6 and $TlBi_2Cl_7$. Journal of Inorganic and General Chemistry / Zeitschrift für anorganische und allgemeine Chemie, 2010, 10.1002/zaac.200900567 . hal-00552437

HAL Id: hal-00552437

<https://hal.science/hal-00552437>

Submitted on 6 Jan 2011

HAL is a multi-disciplinary open access archive for the deposit and dissemination of scientific research documents, whether they are published or not. The documents may come from teaching and research institutions in France or abroad, or from public or private research centers.

L'archive ouverte pluridisciplinaire **HAL**, est destinée au dépôt et à la diffusion de documents scientifiques de niveau recherche, publiés ou non, émanant des établissements d'enseignement et de recherche français ou étrangers, des laboratoires publics ou privés.



**Crystalline and Glassy Phases in the Ternary System
 Tl/Bi/Cl: Synthesis and Crystal Structures of the
 Thallium(I) Chloridobismutates(III) Tl_3BiCl_6 and $TlBi_2Cl_7$**

Journal:	<i>Zeitschrift für Anorganische und Allgemeine Chemie</i>
Manuscript ID:	zaac.200900567.R1
Wiley - Manuscript type:	Article
Date Submitted by the Author:	01-Feb-2010
Complete List of Authors:	Beck, Johannes; University of Bonn, Inorganic Chemistry Benz, Sebastian
Keywords:	Thallium, Chloridobismutate, Lone pair effect, 203/205Tl solid state NMR spectra, X-Ray absorption spectra



1
2
3
4
5
6
7
8 **Crystalline and Glassy Phases in the Ternary System Tl/Bi/Cl: Synthesis**
9 **and Crystal Structures of the Thallium(I) Chloridobismutates(III) Tl_3BiCl_6**
10 **and $TlBi_2Cl_7$**
11
12
13
14
15
16
17
18

19 **Johannes Beck***^[a] and **Sebastian Benz**^[a]
20
21
22
23
24

25 Bei der Redaktion eingegangen am.....
26
27
28
29

30 Dedicated to Professor Rüdiger Kniep on the occasion of his 65th birthday
31
32
33
34
35
36
37
38
39
40
41
42
43
44
45

46
47
48 *Prof. Dr. J. Beck
49

50 e-mail: j.beck@uni-bonn.de
51

52 [a] Universität Bonn, Institut für Anorganische Chemie
53

54 Gerhard-Domagk-Str. 1, D-53121 Bonn
55
56
57
58
59
60

1
2
3
4
5 **Abstract.** Slow cooling of melts composed of TlCl and BiCl₃ allows for the isolation of the
6 compounds Tl₃BiCl₆ (**1**) and TlBi₂Cl₇ (**2**). **1** is formed by sublimation at 480 °C from the black
7 melt of 3 TlCl + 1 BiCl₃ as colourless crystals. The crystal structure determination (tetragonal,
8 *P4₂/m*) consists of nearly regular octahedral [BiCl₆]³⁻ anions and two independent Tl⁺ cations
9 which have coordination number 8 in form of a slightly distorted cube and 10 in form of an
10 Edshamar polyhedron, respectively. The structure is not isotypic with the recently reported
11 naturally occurring form of Tl₃BiCl₆, the mineral steropesite. **2** is obtained from a dark brown
12 melt of composition TlCl + 2 BiCl₃. On rapid cooling, this melt solidifies to a metastable dark
13 red glass which at ambient temperature crystallizes to a light amber crystalline powder within
14 some weeks. The structure of **2** was determined by powder diffraction (triclinic, *P* $\bar{1}$). A
15 distinct lone pair effect is present causing an irregular coordination on the two independent Bi
16 atoms. Taking Bi–Cl bonds up to 3.5 Å into account, both Bi atoms gain coordination number
17 seven. ²⁰³Tl and ²⁰⁵Tl solid state NMR and XANES spectra on the Bi and Tl-L_{III} edges of both
18 glassy and crystalline TlBi₂Cl₇ show that a close structural similarity exists between both
19 forms. In contrast, the Raman spectra show distinct differences in the bands of the Bi–Cl
20 vibrations region.
21
22
23
24
25
26
27
28
29
30
31
32
33
34
35
36
37
38
39
40
41
42
43
44
45
46
47
48
49
50
51
52
53

54 **Keywords:** Thallium, Chloridobismutate, Lone pair effect, ^{203/205}Tl solid state NMR spectra,
55 X-Ray absorption spectra, Glass formation, X-Ray powder diffraction
56
57
58
59
60

Introduction

The crystal chemistry of the halides of trivalent bismuth is strongly influenced by the stereochemical activity of the lone electron pair on Bi^{3+} . Its structural influence is generally strong among the fluorides, but decreases with the heavier halogens. In the structure of BiF_3 , the Bi^{3+} ion has a distorted square-antiprismatic coordination [1]. In BiCl_3 , a strongly distorted 3+3 octahedral coordination with three short and three long Bi-Cl bonds is present [2], whereas for BiI_3 an almost undistorted octahedral coordination environment was found [3]. During the last two decades, a number of alkali halogenidobismutates have been characterized, which show a large structural variability, mainly caused by the absence or presence of the lone-pair effect of the trivalent bismuth atoms. Examples are CsBi_2F_7 [4] containing a Bi/F framework, in which the bismuth atoms have a strongly distorted six to eight fold coordination by fluoride anions. On the other hand, the structure of Cs_3BiCl_6 [5] contains discrete BiCl_6 units in which the Bi-Cl coordination is nearly ideally octahedral.

This structural variability can be further expanded by the substitution of alkali ions by such ions which themselves have a potentially sterical active lone-pair. Looking for substances with nonlinear optical properties, *Hagemann* and *Weber* prepared crystals of the compounds $\text{Tl}_7\text{Bi}_3\text{I}_{16}$ and Tl_3BiI_6 . The crystal structures, however, could not be determined due to twinning problems [6]. Later, *Ruck* and co-workers were able to characterize structurally the phases $\text{Tl}_7\text{Bi}_3\text{I}_{16}$, Tl_3BiI_6 [7], and $\text{Tl}_3\text{Bi}_2\text{I}_9$ [8] by X-Ray diffraction. All three iodidobismutates have Bi in sixfold coordination. The BiI_6 coordination octahedra are distorted, which is assigned to the effect of the lone pair.

Only one compound in the ternary system Tl/Bi/Cl was described so far. The mineral steropesite of the approximated formula Tl_3BiCl_6 was recently found in volcanic high-temperature fumaroles [9]. The lack of knowledge on this ternary system led us to explore the formation and structures of phases among the thallium chloridobismutates.

Experimental Section

Starting Materials

BiCl_3 was obtained by chlorination of bismuth at 400 °C followed by several cycles of sublimation in vacuum. TlCl was precipitated from an aqueous solution of TlNO_3 with hydrochloric acid, washed with water and dried in dynamic vacuum for several days. Glass ampoules of 10 cm length and 1.5 cm diameter were used as reaction vessels. All

1
2
3 manipulations with the hygroscopic BiCl₃ including charging and opening of the reaction
4 ampoules were performed in an argon filled glove box.
5
6
7

8 *Synthesis of Tl₃BiCl₆*

9
10
11 Tl₃BiCl₆ was synthesized by heating a melt of TlCl and BiCl₃ in 3:1 molar ratio to 480 °C for
12 ten hours in evacuated glass ampoules and slow cooling (5 °C h⁻¹) the black-brown melt to
13 ambient temperature. In a typical experiment, an ampoule of 12 cm length and 1.5 cm
14 diameter was loaded with 700 mg of the TlCl/BiCl₃ mixture. Besides a black amorphous
15 residue, colourless crystals of high refractivity deposited at the inner walls of the ampoule in
16 the cooler region above the melt.
17
18
19
20
21
22

23 *Synthesis of TlBi₂Cl₇*

24
25
26 Polycrystalline samples of TlBi₂Cl₇ were prepared by heating a mixture of TlCl and BiCl₃ in
27 the molar ratio 1:2 to 250 °C in evacuated glass ampoules and slowly cooling (10 °C h⁻¹) the
28 dark red melt to ambient temperature. Trying to obtain single crystals by sublimation of the
29 product only lead to sublimation of BiCl₃ leaving behind the less volatile TlCl.
30
31
32
33
34
35

36 *Analytical Methods*

37
38
39 Raman spectra were recorded using a BRUKER FT Raman spectrometer RFS100 in
40 backscattering geometry, a Nd:YAG laser ($\lambda = 1036$ nm) and a resolution of 4 cm⁻¹. The laser
41 power was adjusted between 30 and 300 mW. Measurements were done on powdered samples
42 enclosed in sealed glass capillaries of 1 mm diameter. X-ray absorption spectra were
43 measured at the synchrotron light source ANKA of the Forschungszentrum Karlsruhe,
44 Germany. Solid state NMR spectra were recorded with a VARIAN Infinity Plus spectrometer
45 applying the MAS technique. Samples were packed in a rotor of 4 mm diameter and a rotation
46 frequency of 12 kHz was applied. The spectrum was calibrated against a solution of TlNO₃
47 with a concentration of 0.1 mol L⁻¹. The resonance frequencies were 229.36 MHz for ²⁰³Tl
48 and 231.62 MHz for ²⁰⁵Tl. Differential scanning calorimetry measurements were carried out
49 with a DSC 204 Phoenix instrument (Netzsch Inc.) in closed aluminium crucibles with
50 samples of about 15 mg.
51
52
53
54
55
56
57
58
59
60

Crystal Structure Determination of Tl_3BiCl_6

The crystals of Tl_3BiCl_6 , deposited from the gas phase as described above, were notoriously multiple twinned with diffraction patterns that could not be indexed and it took several attempts until a suitable single crystal specimen was found. Diffraction data were recorded at ambient temperature using a Bruker Nonius Kappa-CCD diffractometer with Mo- K_α radiation. The tetragonal symmetry and the systematic absences led to the space group $P4_2/m$. An empirical absorption correction was applied to the data set [10]. The structure model was obtained by direct methods and refined based on F^2 with anisotropic displacement parameters for all atoms [11]. The crystallographic data and details of data collection are summarized in Tab. 1, atomic coordinates in Tab. 2. The powder diffractograms of bulk samples can, however, be completely indexed and simulated on the basis of the tetragonal unit cell and the positional parameters obtained by the single crystal structure analysis. No reflections of additional phases are present indicating that under the applied reaction conditions only one single phase is formed.

Crystal Structure Determination of $TlBi_2Cl_7$

To protect the slightly hygroscopic powder of $TlBi_2Cl_7$ from moisture, samples were filled in glass capillaries with a diameter of 0.2 mm after thoroughly grinding with an equal amount of glass powder. Data were collected at ambient temperature using a Bruker-D8 Advance powder diffractometer with Cu- K_α radiation. 10482 data points were recorded in the 2θ range 4 to 81° with increments of 0.00735° . Indexing of the diffractogram and determination of the lattice parameters was performed using the program WinXPow [12]. The diffraction pattern could be indexed by a triclinic cell. A first kind Chebyshev background function with 30 terms was applied as implemented in the GSAS program system [13]. A Pseudovoigt function with 18 terms was used to fit the reflection profiles for all 1480 identified reflections. Structure models were obtained with the aid of the program Endeavour [14]. Due to the closely similar atom scattering factors of Bi and Tl, it turned out to be advantageous to assume both kinds of atoms as occupied by Pb in the structure solution process and in the early stages of refinement. Out of the suggested structure models those were chosen fulfilling the restraints $d_{\min}(\text{Pb-Pb}) = 3,5\text{\AA}$, $d_{\min}(\text{Pb-Cl}) = 2,5\text{\AA}$, $d_{\min}(\text{Cl-Cl}) = 3,0\text{\AA}$. Eliminating all models with high coordination numbers of cations by cations or anions by anions, one centrosymmetric model was left, which was refined by the Rietveld method using the program GSAS [12]. Finally, an assignment of the different Tl and Bi positions could be

1
2
3 made unequivocally based on the respective cation–Cl bond lengths. Isotropic displacement
4 parameters for all atoms were chosen and refined as free parameters. Table 1 contains the
5 crystallographic data and details of the refinement, Table 3 the positional parameters of the
6 atoms. Fig.1 shows the observed the calculated powder diffractogram.
7
8
9

10
11 Further crystallographic data for both crystal structure determinations have been deposited
12 with the *Fachinformationszentrum Karlsruhe* under the deposit numbers CSD-421317 for
13 Tl_3BiCl_6 and CSD-421318 for TlBi_2Cl_7 [15]. The graphical representations were drawn with
14 the use of the programs DIAMOND [16] and POV-RAY [17].
15
16
17
18
19

20 21 **Results and Discussion**

22 23 *Synthesis of Thallium (I) Chloridobismutates*

24
25
26
27
28 In a series of experiments, the formation of discrete phases in the ternary system Tl/Bi/Cl was
29 investigated by reactions of TlCl and BiCl_3 in different molar ratios from 3 : 1 to 1 : 3. With
30 intermediate compositions no formation of compounds was observed. Powder diffractograms
31 of solidified melts of compositions between 2 : 1 and 1 : 1 showed beside reflections of new
32 phases reflections of the starting materials TlCl and BiCl_3 . Another common feature is the
33 widespread formation of dark coloured glassy solids on solidification of the melts. The
34 formation of ternary compounds was only observed on the border areas of the investigated
35 compositions, in the thallium rich and the bismuth rich region. Two different thallium(I)
36 chloridobismutates, Tl_3BiCl_6 and TlBi_2Cl_7 , composed of TlCl and BiCl_3 in the stoichiometric
37 amounts 3 : 1 and 1 : 2, could be synthesized and isolated as discrete phases. With both
38 compositions as a typical feature dark coloured melts are formed. In the case of the 3 : 1
39 mixture, the deposition of crystals of Tl_3BiCl_6 from the gas phase above the melt in a small
40 temperature gradient during the slow cooling process from 480 °C to ambient temperature
41 could be achieved. The deposited colourless crystals of Tl_3BiCl_6 are strongly light refracting.
42 The analogous experiments with melts of the composition 1 TlCl : 2 BiCl_3 gave melts of dark-
43 red colour. In contrast to the TlCl rich melts, no deposition of crystalline material was
44 observed from the gas phase above the melts of this composition. Slow cooling of such a melt
45 from 250 °C to ambient temperature gives an amber coloured microcrystalline solid. By rapid
46 quenching the melt from 250 °C to –38 °C, performed by immersing the hot reaction ampoule
47 into chilled liquid mercury, an amorphous, glassy, transparent, dark-red product was isolated
48
49
50
51
52
53
54
55
56
57
58
59
60

(Fig. 2a). Grinding of the red glass gives a light red to rose powder. The non-crystallinity was verified by X-Ray powder diffraction. Leaving this glassy material at room temperature under protection from moist air causes the slow conversion into the light amber coloured crystalline phase (Fig. 2b).

Crystal Structure of Tl_3BiCl_6

The tetragonal unit cell of Tl_3BiCl_6 contains two formula units (Fig. 3). Two Bi atoms occupying the site symmetry $2/m$ are almost regular octahedrally coordinated by six Cl atoms. The two independent Bi–Cl distances are equal within standard deviations and amount 2.692(2) and 2.693(3) Å (Tab. 4). The angular distortions within the $BiCl_6$ octahedra are small. A significant deviation from rectangularity is observed for the plane containing the Bi atoms and the four Cl(1) atoms, which is inclined by 3° to the Cl(2)–Bi–Cl(2^{II}) axis. An almost regular shape of $BiCl_6$ octahedra in the structures of chloridobismutates(III) is not unusual and found e.g. in the structure of $(NH_4)_3[BiCl_6]$ (Bi–Cl 2.682 to 2.753 Å, angle deviations from 90° less than 6°) [18].

The tetragonal unit cell of Tl_3BiCl_6 contains two independent thallium atoms. The coordination sphere around the Tl(1) atoms, located on the *Wyckoff* site $4j$ in the mirror plane may be described best by a distorted *Edshamar* polyhedron with coordination number of 10 and Tl–Cl distances in the region between 3.117(3) to 3.802(3) Å, formally built by half a cube and half an icosahedron. Tl(2) atoms with site symmetry $2/m$ are surrounded by eight chlorine atoms in shape of a cube. The actual reduction of the ideal cubic symmetry to $2/m$ allows for distortions which find their expressions in two different Tl–Cl distances of 3.281(3) and 3.312(3) Å. The cuboidal Tl(2)Cl₈ polyhedra are condensed to linear strands along the crystallographic *c* axis with the Tl ions being half the length of the *c* axis (3.744 Å) apart. The Tl(1)Cl₁₀ polyhedra share two of their square faces and four edges with the Tl(2)Cl₈ polyhedra resulting in a three-dimensional network (Fig. 3).

Since Tl_3BiCl_6 is of the basic formula type A_3BX_6 , for which numerous representatives are known, we attempted to contribute its structure to a known structure type. The actual release of the ICSD database [19] contains 479 known crystal structures of this formula type. Using the subroutine CMPZ of the program KPLOT [20] a similarity search was performed. The tolerances were set to high values: for all lattice constants a tolerance of $\pm 15\%$, for deviation

1
2
3 of angles $\pm 5\%$, the inclusion spheres for atom positions were enlarged to 1.0 Å. Surprisingly
4 and despite the wide tolerances, no coincidence with any of the deposited structures of the
5 A_3BX_6 formula type compounds was found. The arrangement of the Tl^+ ions in rows along
6 one crystallographic axis with the remarkably short $Tl^+ \cdots Tl^+$ distances is unusual and causes
7 the uniqueness of Tl_3BiCl_6 within the structures of this formula type.
8
9

10
11
12
13
14 The recently described mineral steropesite was discovered as yellow crystals of the formula
15 Tl_3BiCl_6 [9]. The structure was solved on a crystal containing 10 % Br on the Cl positions. It
16 crystallizes in the monoclinic system with a very large unit cell having a volume of almost
17 5000 \AA^3 . Its crystal structure consists of discrete and slightly distorted octahedral $[BiCl_6]^{3-}$
18 anions and Tl^+ cations with coordination numbers between six and eight. The reported
19 structure can be considered as a distorted variant of the structure of Cs_3BiCl_6 , but besides the
20 presence of the analogous building units there is no direct relation to the tetragonal form of
21 Tl_3BiCl_6 reported here.
22
23
24
25
26
27

28 29 *The High Temperature Phase of Tl_3BiCl_6*

30
31
32
33 The thermal behaviour of Tl_3BiCl_6 was investigated in the temperature region between
34 ambient temperature and 400 °C by differential scanning calorimetry at a heating rate of 10
35 °C min^{-1} . Two reproducible, endothermic effects could be detected, a solid state phase
36 transition at 189.1 °C (0.93 kJ mol^{-1}), and the melting at 378.4 °C (3.4 kJ mol^{-1}). To test for a
37 transition into a high temperature form, crystals of the low temperature form were grinded to
38 a powder, filled into a glass capillary, which was sealed, and investigated by X-ray powder
39 diffractometry. Above 230 °C the diffraction pattern changed completely and the reflections
40 of the room temperature phase disappeared. Lowering the temperature again to 180 °C caused
41 only an incomplete reversion since the diffractogram of the room temperature phase
42 appeared again but the strongest reflections of the high temperature diffractogram remained.
43 The powder diffractogram at high temperature shows a significant higher number of
44 reflections. This behaviour may indicate a transition to a high temperature phase with a
45 structure of lower symmetry. On looking for a structure model for the assumed high
46 temperature phase, we found that the calculated powder diffractogram of monoclinic
47 Cs_3BiCl_6 , after substitution of Cs against Tl, shows a striking similarity to the diffractogram
48 of HT- Tl_3BiCl_6 . The complete indexing of the diffractogram was not successful and a
49 refinement of the structure model was not possible on basis of the observed diffraction data.
50 We cannot, however, rule out the possibility of a partial decomposition of the sample.
51
52
53
54
55
56
57
58
59
60

Crystal Structure of TlBi₂Cl₇

The triclinic unit cell of TlBi₂Cl₇ contains two formula units with all atoms occupying general positions. The coordination of the two independent Bi atoms and the Tl atom by surrounding Cl atoms is much more irregular in comparison to the structure of Tl₃BiCl₆. In Fig. 4 the distribution of these distances is depicted in the form of histograms. For all three independent cations present in the crystal structure, a distinct gap is observed which allows for the definition of coordination polyhedra. The two Bi atoms both gain coordination number seven with all Bi–Cl distances up to 3.34 Å for Bi(1) and 3.47 Å for Bi(2) taken into account. In each of the two BiCl₇ polyhedra one Cl atom achieves a long distance which is typical for a pronounced lone pair effect of the trivalent Bi atom. The BiCl₇ polyhedra are connected via common corners and edges to a three dimensional net, in which the Tl⁺ ions are embedded. Tl gains the coordination number eleven if all Tl–Cl distances up to 4.09 Å are considered (Fig. 4).

Vibrational Spectra

Of both compounds, Tl₃BiCl₆ and TlBi₂Cl₇, Raman spectra were recorded. As expected, the spectrum of Tl₃BiCl₆ shows only a low number of bands due to the high local symmetry of the vibrational active BiCl₆ group. Three broad bands at 261 (vs), 218 (s), and 117 (vs) cm⁻¹ were observed. These bands are identical with those of Cs₃BiCl₆ within the resolution limit and can be attributed to the fundamental Raman active vibrations A_{1g}, E_g, T_{2g} of the BiCl₆ octahedron. In the region between 300 and 100 cm⁻¹ the Raman spectrum of TlBi₂Cl₇ shows 10 bands (104(s), 116(m), 121(m), 132(s), 144(w), 172(s), 186(s), 247(s), 269(s), 290(s) cm⁻¹). Due to the irregular, low symmetric coordination of the cation in this structure, a definite attribution of these bands cannot be made.

Structural Investigations of the Glassy TlBi₂Cl₇

The thermal behaviour of glassy TlBi₂Cl₇ was measured in the temperature region between -20 and 230 °C, the respective differential scanning calorimetry (DSC) function, obtained at a heating rate of 10 °C min⁻¹ is given in Fig. 5. The endothermic effect at 41.3 °C (point *a* in

1
2
3 Fig. 5, 2.9 kJ mol⁻¹) is attributed to the glass transition. The two following exothermic effects
4 at 59.3 (*b* and *c*, -6.0 kJ mol⁻¹) are attributed to crystallization processes. The small
5 endothermic effect at 180 °C (*d*) was not observable in all measurements and is probably an
6 artefact. At 189.5 °C melting occurs (*e*, 30.3 kJ mol⁻¹). On cooling the samples after melting,
7 a sharp exothermic signal at 109 °C appears (*f*, -22.1 kJ mol⁻¹) originating from
8 crystallization of the melt. If the measurement is carried out with a lower heating rate of 1 °C
9 min⁻¹, the glass transition shifts to 35.2 °C. According to the empirical relation $T_g = A + B$
10 $\log\beta$ with T_g = observed glass transition temperature, A = true glass transition temperature, B
11 = empirical factor depending on the preparation of the glass, β = heating rate, the transition
12 temperature at 32.5 °C is identical with the true transition temperature [21]. The relation of
13 the absolute glass transition temperature to the melting temperature allows within limits for
14 information on the structural properties of amorphous networks. For highly symmetric
15 polymers, made up from small monomeric units, T_g/T_m is generally 0.5 or lower, for the broad
16 majority of polymers, however, this relation amounts 2/3 [22]. For the amorphous TlBi₂Cl₇
17 phase T_g/T_m is 308 K/463 K = 0.66. The observed thermal effects do thus not allow for
18 detailed conclusions on the structural properties of the glass.
19
20
21
22
23
24
25
26
27
28
29
30
31
32

33 ²⁰⁵Tl and ²⁰³Tl MAS solid state NMR spectra were recorded in order to find further insight
34 into the structure of the red glassy form of TlBi₂Cl₇. The MAS spectra of both, the glassy and
35 the crystalline TlBi₂Cl₇ do not show differences. Only one broad signal centered at 47.7 ppm
36 relative to the standard was observed (Fig. 6). This is in line with the crystallographic cell,
37 which contains only one symmetry-independent Tl atom. The similarity of the spectra
38 suggests that the chemical environment of the thallium atoms in both phases does not show
39 large differences.
40
41
42
43
44
45
46
47

48 The vibrational spectrum of the amorphous TlBi₂Cl₇ phase shows, however, distinct
49 differences to the spectrum of the crystalline form. Eight bands (126(s), 142(m), 157(m),
50 178(s), 246(m), 268(w), 292(sh, s), 306(vs) cm⁻¹) are present, of which only three (142, 246,
51 268 cm⁻¹) are observed at the same frequencies as for the crystalline state. The spectrum of
52 amorphous TlBi₂Cl₇ shows instead a close similarity to the spectrum of BiCl₃ (six bands at
53 280(vs), 262(m), 252(sh, w), 179(m), 141(m), 119(m)) in the frequency and intensity
54 distribution. For BiCl₃ the bands at 280 (A₁) and 252 cm⁻¹ (E) can be attributed to the C_{3v}
55 symmetric molecules, which are present in the solid state. The vibrational spectra lead to the
56
57
58
59
60

1
2
3 suggestion that amorphous TlBi_2Cl_7 contains BiCl_3 building units as present in the structure
4 of crystalline BiCl_3 .
5
6
7

8
9 Near edge X-ray absorption spectra (XANES) of Tl_3BiCl_6 , and amorphous and crystalline
10 TlBi_2Cl_7 were recorded on both the Tl-L_{III} and the Bi-L_{III} edges. Fig. 7 shows the spectra on
11 the Bi-L_{III} edges as a superposition for all three samples. A striking similarity is observed
12 between the spectra of glassy and crystalline TlBi_2Cl_7 , while the spectrum of Tl_3BiCl_6 is
13 different throughout the entire energy interval. This observation is also valid for the spectra on
14 the Tl-L_{III} edge. This result is in line with the solid state NMR spectra, indicating that
15 TlBi_2Cl_7 in the glassy and the crystalline state both have closely related coordination
16 environments around the Tl and Bi atoms. On the other hand, the Raman spectra with their
17 differing patterns of vibrational bands indicate a substantially altered local structure.
18
19
20
21
22
23
24
25
26
27

28 **Conclusion**

29
30 Two discrete phases were prepared and characterized in the ternary system Tl/Bi/Cl, both
31 showing structural peculiarities. The TlCl rich compound Tl_3BiCl_6 is built of only slightly
32 distorted $[\text{BiCl}_6]^{3-}$ octahedra, while the BiCl_3 rich phase TlBi_2Cl_7 is made of a complex
33 network of connected, irregular BiCl_7 polyhedra. In both structures, the Tl^+ ions gain high
34 coordination numbers between eight and eleven. A remarkable and yet not elucidated detail is
35 the amorphous state of TlBi_2Cl_7 , which forms a glass on rapid cooling of the melt. The
36 metastable, transparent glass is of intensive dark-red colour, while the crystalline phase is
37 almost colourless. No explanation for the colour of the glass could be found and the attempts
38 to find structural relations between the glassy and the crystalline state by XANES, NMR and
39 Raman spectra lead to contradictory results.
40
41
42
43
44
45
46
47
48
49
50

51 **Acknowledgement**

52
53
54
55 We gratefully acknowledge the measurements of the X-ray absorption spectra by N. Palina,
56 B. Brendebach and H. Modrow, the collection of the single crystal data by J. Daniels, the
57 recording of the NMR spectra by W. Hoffbauer and the dedicated help of R. Hundt with the
58 data base searches.
59
60

Table 1 Crystallographic data and details of the structure determination for Tl_3BiCl_6 and TlBi_2Cl_7 .

Compound	Tl_3BiCl_6	TlBi_2Cl_7
Formula	BiCl_6Tl_3	$\text{Bi}_2\text{Cl}_7\text{Tl}$
Crystal system, space group	tetragonal, $P4_2/m$	triclinic, $P\bar{1}$
Number of formula units, Z	2	2
$a / \text{\AA}$	8.9690(2)	8.8832(1)
$b / \text{\AA}$		10.7632(1)
$c / \text{\AA}$	7.4876(2)	6.9329(1)
$\alpha / ^\circ$		107.523(1)
$\beta / ^\circ$		107.334(1)
$\gamma / ^\circ$		75.684(1)
$V / \text{\AA}^3$	602.32(2)	594.30(1)
Density (calc.)/ $\text{g}\cdot\text{cm}^{-3}$	5.706	4.86
Absorption coefficient μ / mm^{-1}	55.84 (Mo $K\alpha$)	96.89 (Cu $K\alpha$)
Diffractometer type	Bruker-Nonius κ -CCD	Bruker D8 Advance
Radiation, wavelength / \AA	Mo- $K\alpha$, 0.7107	Cu- $K\alpha_1$, 1.540598
Temperature / K	293	293
$2\theta_{\text{max}} / ^\circ$, hkl range	54.94°; $h\pm 11$, $k\pm 8$, $l\pm 9$	$4^\circ < 2\theta < 81^\circ$, $0 \leq h \leq 7$, $-8 \leq k \leq 9$, $-5 \leq l \leq 5$
Absorption correction	empirical [9]	cylinder correction
$T_{\text{min}}/T_{\text{max}}$	0.005/0.065	0.060/0.107
Reflections collected	1356	1484
Independent reflections, R_{merg}	730, 0.027	
No. of data and parameters	730 and 31	1480 and 41
Goodness-of-fit on F^2	1.066	1.55
$wR(F^2)$	0.070	0.043
$R(F)$ for $[n] F_0 > 4\sigma(F_0)$	0.028 [682]	
$R(F)$ for all data	0.031	
R_{Profiles}		0.031
wR_{Profiles}		0.043
$wR(F^2)$		0.079
Largest difference peak and hole / $\text{e}\cdot\text{\AA}^{-3}$	+1.30 and -1.57	1.88 and -1.61

Table 2 Positional coordinates and equivalent isotropic displacement parameters $U_{eq} / \text{\AA}^2$ for the atoms in the structure of Tl_3BiCl_6 . Standard deviations refer to the last significant digit.

Atom	x	y	z	U_{eq}
Tl(1)	0.07685(7)	0.26533(6)	0	0.0540(3)
Tl(2)	0.5	0.5	0	0.0373(3)
Bi	0	0.5	0.5	0.0221(2)
Cl(1)	0.2037(2)	0.5612(3)	0.2463(3)	0.0382(5)
Cl(2)	0.0644(4)	0.2068(4)	0.5	0.059(1)

Table 3 Positional coordinates and isotropic displacement parameters $U_{iso} / \text{\AA}^2$ for the atoms in the structure of TlBi_2Cl_7 . Standard deviations refer to the last significant digit.

Atom	<i>x</i>	<i>y</i>	<i>z</i>	U_{iso}
Tl	0.6739(2)	0.1409(2)	0.9225(3)	0.0437(7)
Bi(1)	-0.2437(2)	0.5188(2)	0.5569(3)	0.0156(5)
Bi(2)	0.1380(2)	0.1583(2)	0.6966(2)	0.0209(6)
Cl(1)	-0.158(1)	0.3547(9)	0.795(1)	0.030(3)
Cl(2)	0.000(1)	0.0194(8)	0.262(1)	0.023(3)
Cl(3)	0.352(1)	0.318(1)	0.705(2)	0.053(4)
Cl(4)	0.256(1)	0.1904(9)	1.094(1)	0.032(3)
Cl(5)	0.370(1)	-0.0332(8)	0.647(1)	0.024(3)
Cl(6)	0.053(1)	0.6431(8)	0.648(1)	0.027(3)
Cl(7)	-0.445(1)	0.3869(9)	0.311(1)	0.028(3)

Table 4 Selected bond lengths / Å in the structures of Tl_3BiCl_6 and TlBi_2Cl_7 . For symmetry operations see legends of Figs. 1 and 2.

Tl_3BiCl_6		TlBi_2Cl_7	
Bi–Cl(1), Cl(1 ^{II}), Cl(1 ^{XIII}), Cl(1 ^{XIV})	2.692(2)	Bi(1)–Cl(1)	2.603(9)
Bi–Cl(2), Cl(2 ^{II})	2.693(3)	Bi(1)–Cl(3 ^{II})	2.705(9)
Tl(1)–Cl(1), Cl(1 ^{IV})	3.426(3)	Bi(1)–Cl(4 ^I)	3.331(9)
Tl(1)–Cl(1 ^{II}), Cl(1 ^{III})	3.486(3)	Bi(1)–Cl(6)	3.059(9)
Tl(1)–Cl(1 ^I), Cl(1 ^V)	3.802(3)	Bi(1)–Cl(6 ^{II})	2.533(9)
Tl(2)–Cl(1), Cl(1 ^{IV}), Cl(1 ^{IX}), Cl(1 ^{XI})	3.281(3)	Bi(1)–Cl(7)	2.470(9)
Tl(2)–Cl(1 ^I), Cl(1 ^V), Cl(1 ^X), Cl(1 ^{XII})	3.312(3)	Bi(1)–Cl(7 ^{III})	3.010(9)
		Bi(2)–Cl(1)	3.048(10)
		Bi(2)–Cl(2)	2.967(8)
		Bi(2)–Cl(2 ^{IV})	2.636(8)
		Bi(2)–Cl(3)	2.845(10)
		Bi(2)–Cl(4)	2.584(9)
		Bi(2)–Cl(5)	2.551(8)
		Bi(2)–Cl(6 ^{II})	3.467(9)
		Tl – Cl	3.374(9) to 4.087(9)

References

- 1
2
3
4
5
6
7
8 [1] O. Greis, M. Martinez-Ripoll, *Z. Anorg. Allg. Chem.* **1977**, 436, 105.
9
10 [2] S. C. Nyburg, G. A. Ozin, J. T. Szymanski, *Acta Crystallogr.* **1972**, B28, 2885.
11
12 [3] M. Ruck, *Z. Kristallogr.* **1995**, 210, 650.
13
14 [4] A. M. Golubev, B. A. Maksimov, R. K. Rastsvetaeva, *Crystallogr. Reports*
15 **1997**, 42, 243.
16
17 [5] F. Benachenhou, G. Mairesse, G. Nowogrocki, D. Thomas, *J. Solid State Chem.*
18 **1986**, 65, 13.
19
20 [6] M. Hagemann, H. J. Weber, *Appl. Phys.* **1996**, A63, 67.
21
22 [7] T. Aussieker, H. L. Keller, T. Oldag, Y. Prots, M. Ruck, A. Wosylus, *Z. Anorg.*
23 *Allg. Chem.* **2007**, 633, 603.
24
25 [8] A. Wosylus, U. Schwarz, M. Ruck, *Z. Anorg. Allg. Chem.* **2005**, 631, 1055.
26
27 [9] F. Demartin, C. M. Gramaccioli, I. Campostrini, *Canad. Mineralog.* **2009**, 47,
28 373.
29
30 [10] Z. Otwinowski, W. Minor, Program SCALEPACK, *Macromol. Crystallogr. A*
31 **1997**, 276, 307.
32
33 [11] G. M. Sheldrick, *SHELX97 [includes SHELXS97, SHELXL97, CIFTAB] -*
34 *Programs for Crystal Structure Analysis (Release 97-2)*. Universität Göttingen,
35 Germany, 1998.
36
37 [12] *WinXPow*, Powder Diffraction Software, Stoe & Cie Ltd., Darmstadt, Germany,
38 1999.
39
40 [13] *General Structure Analysis System (GSAS)*, A. C. Larson, R. B. Von Dreele,
41 Los Alamos National Laboratory, Report LAUR 86-748 (2000).
42
43 [14] *ENDEAVOUR, Program for Structure Solution from Powder Diffraction*,
44 Crystal Impact GbR, Bonn, Germany; H. Putz, J.C. Schoen, M. Jansen, *J. Appl.*
45 *Cryst.* **1999**, 32, 864.
46
47 [15] Detailed crystallographic data can be obtained from the
48 *Fachinformationszentrum Karlsruhe* by quoting the deposit number, the names
49 of the authors and the literature citation. Details about inquiries are given on
50 *www.fizinformationsdienste.de*.
51
52 [16] *DIAMOND, Molecular and Crystal Structure Visualization Program*, ver. 3.1,
53 Crystal Impact GbR, Bonn, Germany, 2008.
54
55
56
57
58
59
60

- 1
2
3 [17] POV-Ray, Persistence of Vision Raytracer Pty. Ltd., Williamstown, Australia
4 (2004).
5
6 [18] I. Belkhal, R. Mokhlisse, B. Tanouti, K. F. Hesse, W. Depmeier, *Europ. J. Solid*
7 *State Inorg. Chem.* **1997**, *34*, 1085.
8
9 [19] *Inorganic Crystal Structure Database ICSD*, Fachinformationszentrum FIZ
10 Karlsruhe, Germany, Release 2009-1.
11
12 [20] *KPLOT, Program for Graphical Representation and Analysis of Crystal*
13 *Structures*, R. Hundt, University of Bonn, Germany, 2007.
14
15 [21] A. A. Othman, K. A. Aly, A. M. Abousehly, *Solid State Comm.* **2006**, *138*, 184.
16
17 [22] H. K. Cammenga, M. Epple, *Angew. Chem.* **1995**, *107*, 1284; *Int. Ed.* **1995**, *34*,
18 1171.
19
20
21
22
23
24
25
26
27
28
29
30
31
32
33
34
35
36
37
38
39
40
41
42
43
44
45
46
47
48
49
50
51
52
53
54
55
56
57
58
59
60

Legends for Figures

Fig. 1 Powder diffractogram of TlBi_2Cl_7 . Shown are the measured intensities, the calculated intensities, the background function, and the difference curve $I_{\text{obs}}-I_{\text{calc}}$. The inset shows an enlarged view of the high angle region of the diffractogram.

Fig. 2 Photographs of pieces of the rapidly cooled melt of TlBi_2Cl_7 , forming a dark red, transparent glass (a), and this glass after two weeks at room temperature with emerging amber coloured crystalline segregations (b).

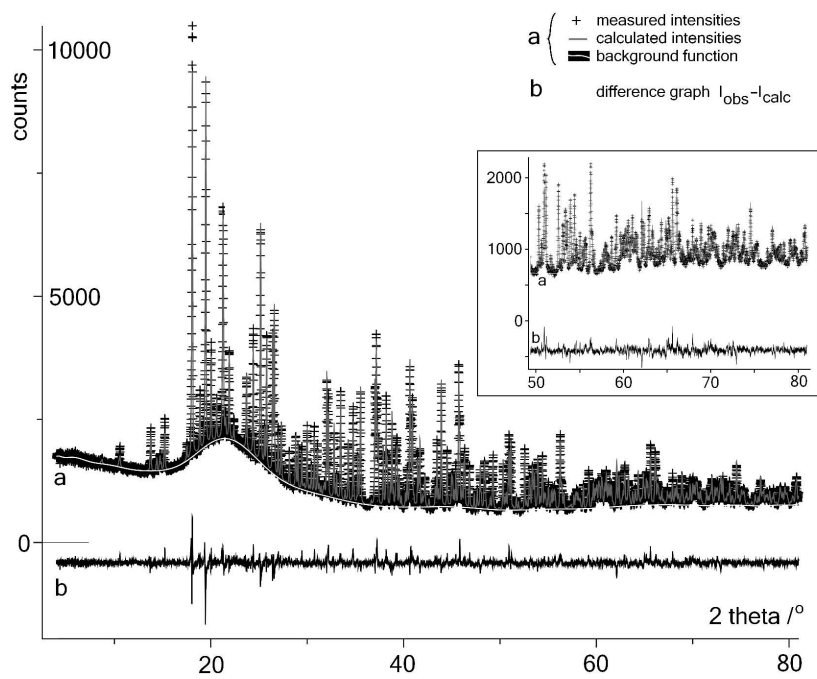
Fig. 3 Details of the crystal structure of Tl_3BiCl_6 (from top to bottom): The coordination polyhedra of the two independent Tl^+ ions $\text{Tl}(1)$ and $\text{Tl}(2)$, the octahedral $[\text{BiCl}_6]^{3-}$ anion, and a view of the unit cell along the crystallographic c axis. Thermal ellipsoids are drawn to include a probability density of 50%. Symmetry operations: I: $1-y, x, -0.5+z$; II: $-x, 1-y, z$; III: $-x, 1-y, -z$; IV: $x, y, -z$; V: $1-y, x, 0.5-z$; VI: $x, y, -1+z$; VII: $-y, x, -0.5+z$; VIII: $y, -x, -0.5+z$; IX: $1-x, 1-y, z$; X: $y, 1-x, -0.5+z$; XI: $1-x, 1-y, -z$; XII: $y, 1-x, 0.5-z$; XIII: $-x, 1-y, 1-z$; XIV: $x, y, 1-z$

Fig. 4 Details of the crystal structure of TlBi_2Cl_7 (from top to bottom): The Bi–Cl and Tl–Cl distances in the form of histograms, the coordination polyhedron of the Tl^+ ion, the coordination of the two independent Bi atoms $\text{Bi}(1)$ and $\text{Bi}(2)$, and a view of the unit cell along the crystallographic c axis. In the two detailed representations, atoms are drawn as spheres with radii corresponding to 50 % of the probability density of the thermal vibration. Symmetry operations: I: $-x, 1-y, 2-z$; II: $-x, 1-y, 1-z$; III: $-1-x, 1-y, 1-z$; IV: $-x, -y, 1-z$; V: $1+x, y, 1+z$; VI: $1-x, -y, 1-z$; VII: $1-x, -y, 2-z$; VIII: $1+x, y, z$; IX: $1-x, 1-y, 2-z$.

Fig. 5 Differential scanning calorimetry function of TlBi_2Cl_7 . The solid line represents the heating curve from -10 to 210 °C, the dotted line the cooling process back to ambient temperature. The observable thermal effects are indicated by letters a-f, see text. The temperature rate for heating (T up) and for cooling (T down) was 10 °C min^{-1} .

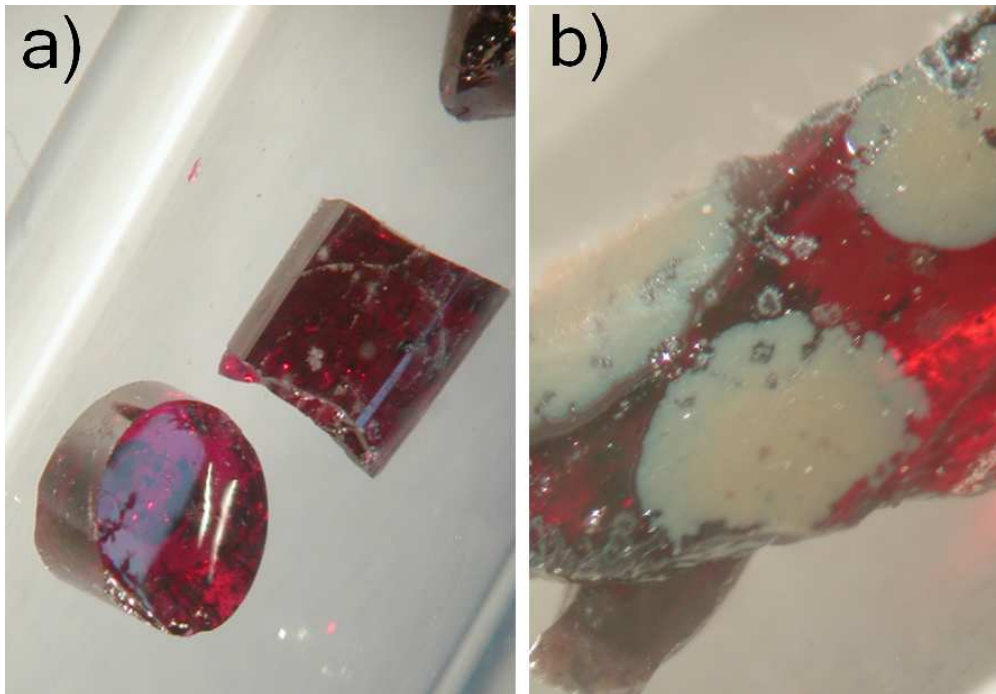
1
2
3 **Fig. 6** ^{205}Tl MAS-NMR spectrum of amorphous TlBi_2Cl_7 at 12 kHz spinning speed. Signals
4 marked with an asterisk are rotational bands. The respective ^{203}Tl spectrum is of almost
5 identical shape but shows lower signal intensity.
6
7
8
9

10
11
12 **Fig. 7** XANES spectrum on the Bi-L_{III} absorption edge of glassy and crystalline TlBi_2Cl_7 ,
13 and of crystalline Tl_3BiCl_6 .
14
15
16
17
18
19
20
21
22
23
24
25
26
27
28
29
30
31
32
33
34
35
36
37
38
39
40
41
42
43
44
45
46
47
48
49
50
51
52
53
54
55
56
57
58
59
60

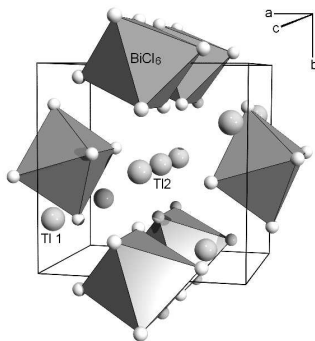
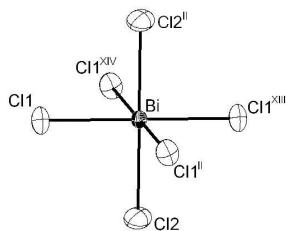
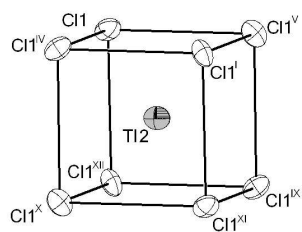
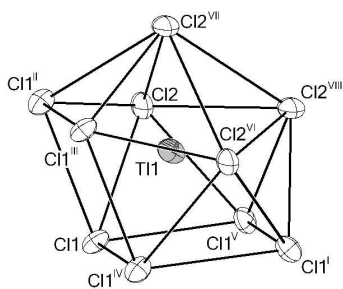


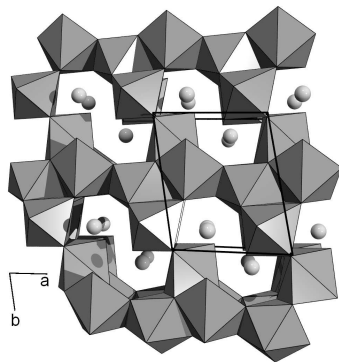
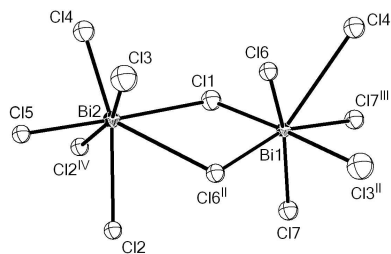
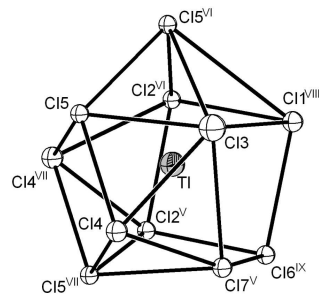
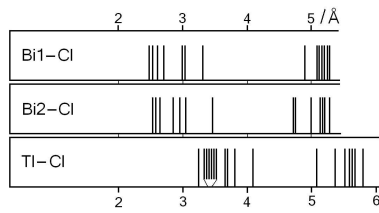
1438x1016mm (72 x 72 DPI)

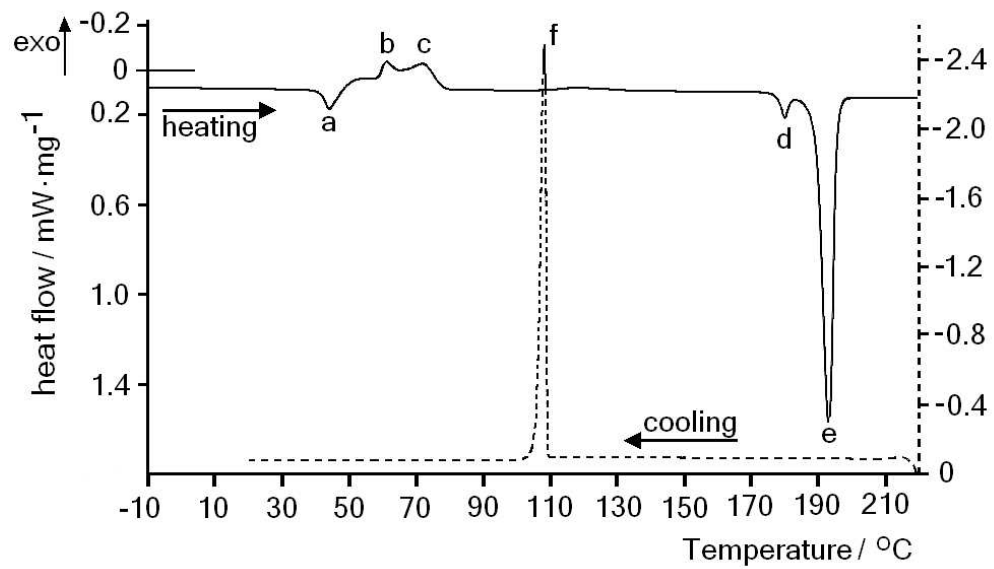
1
2
3
4
5
6
7
8
9
10
11
12
13
14
15
16
17
18
19
20
21
22
23
24
25
26
27
28
29
30
31
32
33
34
35
36
37
38
39
40
41
42
43
44
45
46
47
48
49
50
51
52
53
54
55
56
57
58
59
60



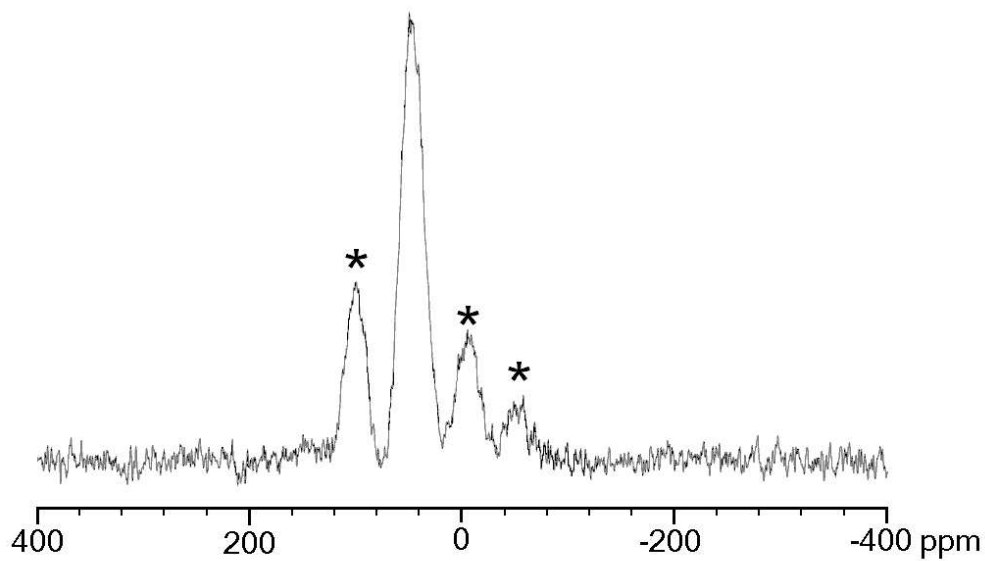
235x162mm (96 x 96 DPI)



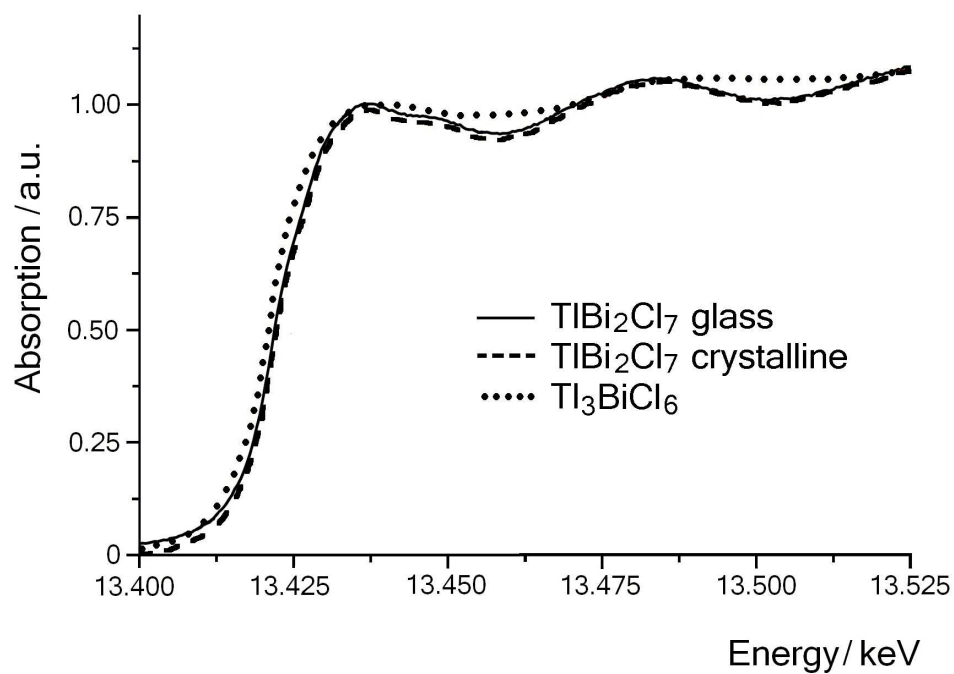




260x160mm (96 x 96 DPI)



86x51mm (300 x 300 DPI)



480x333mm (96 x 96 DPI)